Structure-Based Design of an Inhibitor of the Zinc Peptidase Thermolysin

Bradley P. Morgan,‡ Debra R. Holland,† Brian W. Matthews,† and Paul A. Bartlett*,‡

Contribution from the Department of Chemistry, University of California, Berkeley, California 94720, and Institute of Molecular Biology and Howard Hughes Medical Institute, University of Oregon, Eugene, Oregon 97403

Received August 6, 1993®

Abstract: The full cycle of design, synthesis, and enzymatic and crystallographic evaluation of a structure-based inhibitor of thermolysin is described. Using the structure of the complex of thermolysin with Cbz-Gly^P-Leu-Leu (K_i = 9 nM; "Gly^P" = $NHCH_2PO_2^-$) as the starting point, we designed the macrocyclic phosphonamidate (*S,S*)-**1** as a conformationally constrained derivative. The chroman linking unit was designed to rigidify the peptide analog while avoiding unfavorable steric interactions with the enzyme. (*S,S*)-**1** was synthesized by a route that provided all of the stereoisomers in pure form; the acyclic control compounds **2** and **3** were also prepared. The binding affinity of (*S,S*)-**1** (K_i = 4 nM) is enhanced by 2.3 kcal/mol in comparison to **3** (K_i = 190 nM); the other diastereomers of **1** are considerably less potent ($K_i \geq 500$ nM). Crystallographic analysis of the complexes between thermolysin and (*S,S*)-**1** and (*S*)-**2** demonstrated that the anticipated mode of binding of (*S,S*)-**1** was fundamentally correct, while revealing some discrepancies with the original model. The structural studies also showed that the chroman moiety in the acyclic analog (*S*)-**2** binds in a different orientation than in the macrocycle, an observation that is important for interpreting the differences in affinity between the macrocyclic inhibitor and the control compounds.

Traditional approaches to the "rational" design of enzyme inhibitors have usually been founded on an understanding of the mechanism of the catalyzed reaction, as exemplified by the transition-state analog[1] and suicide inhibitor[2] strategies. Recently, advances in structural biology, computer graphics, and theory have stimulated approaches to the design of biologically active compounds based on structural, rather than mechanistic considerations.[3] These strategies not only rely on the increasing availability of protein crystal structures and of NMR structures of bound and free ligands but also build on the growing body of information on the changes in binding energy that result from specific alterations in the structure or conformational properties of small molecule inhibitors or protein binding sites.[4,5] This information is most useful when the structural consequences and theoretical implications of such alterations can be verified.

A central tenet in structure-based design is that the binding affinity of a ligand will be improved if its conformational motion can be restricted to that of the bound state.[4a,b] Provided that the structural elements that impose this restriction do not introduce additional, unfavorable interactions, there will be a comparatively smaller entropy loss on binding the constrained analog and a more favorable free energy change as a result. Estimations of the advantage to be gained by constraining a freely rotating bond are complicated by choice of suitable control compounds and vary with the system analyzed, but appear to be on the order of 1.2–1.6 kcal/mol at room temperature.[6] A further consequence of enhancing the binding of an inhibitor through cyclization is the potential for reducing its size; a small inhibitor may make up from cyclization what it loses from removal of a side chain or subunit.

Aside from the inherent attraction of a novel approach to a longstanding problem, structure-based design offers potential solutions to some of the challenges encountered in optimizing the biological activity of peptides and peptide analogs. The use of peptides as lead compounds cannot progress without the development of methods for maximizing their binding affinity, altering their receptor selectivity, and reducing their susceptibility to metabolic degradation. These goals are frequently sought and sometimes achieved through classical approaches to cyclic peptides,[7] although it is not often the case that the cyclization is

† University of Oregon.
‡ University of California.
® Abstract published in *Advance ACS Abstracts,* February 1, 1994.

(1) Wolfenden, R. *Annu. Rev. Biochem. Bioeng.* **1976**, *5*, 271–306. Stark, G. R.; Bartlett, P. A. *Pharmacol. Ther.* **1983**, *23*, 45–78. Frick, L.; Wolfenden, R. In *Design of Enzyme Inhibitors as Drugs*; Sandler, M., Smith, H. J., Eds.; Oxford University Press: New York, 1989; pp 19–48.

(2) Walsh, C. *Tetrahedron* **1980**, *38*, 871–909. Silverman, R. B. *Mechanism Based Enzyme Inactivation*; CRC Press: Boca Raton, FL, 1988; Vols 1 & 2.

(3) *Inter alia*: Reich, S. H.; Fuhry, M. A. M.; Nguyen, D.; Pino, M. J.; Welsh, K. M.; Webber, S.; Jannson, C. A.; Jordan, S. R.; Matthews, D. A.; Smith, W. W.; Bartlett, C. A.; Booth, C. L. J.; Herrmann, S. M.; Howland, E. F.; Morse, C. A.; Ward, R. W.; White, J. *J. Med. Chem.* **1992**, *35*, 847–858. Varney, M. D.; Marzoni, G. P.; Palmer, C. L.; Deal, J. G.; Webber, S.; Welsh, K. M.; Bacquet, R. J.; Bartlett, C. A.; Morse, C. A.; Booth, C. L. J.; Herrmann, S. M.; Howland, E. F.; Ward, R. W.; White, J. *J. Med. Chem.* **1992**, *35*, 663–76. Thompson, W. J.; Fitzgerald, P. M. D.; Holloway, M. K.; Emini, E. A.; Darke, P. L.; McKeever, B. M.; Schleif, W. A.; Quintero, J. C.; Zugay, J. A.; et al. *J. Med. Chem.* **1992**, *35*, 1685–1701. Dreyer, G. B.; Lambert, D. M.; Meek, T. D.; Carr, T. J.; Tomaszek, T. A., Jr.; Fernandez, A. V.; Bartus, H.; Cacciavillani, E.; Hassell, A. M.; et al. *Biochemistry* **1992**, *31*, 6646–6659. Ealick, S. E.; Babu, Y. S.; Bugg, C. E.; Erion, M. D.; Guida, W. C.; Montgomery, J. A.; Secrist, J. A., III *Proc. Nat. Acad. Sci. U.S.A.* **1991**, *88*, 11540–11544. DesJarlais, R. L.; Seibel, G. L.; Kuntz, I. D.; Furth, P. S.; Alvarez, J. C.; Ortiz de Montellano, P. R.; DeCamp, D. L.; Babe, L. M.; Craik, C. S. *Proc. Natl. Acad. Sci. U.S.A.* **1990**, *87*, 6644–6648. Kempf, D. J.; Norbeck, D. W.; Codacovi, L.; Wang, X. C.; Kohlbrenner, W. E.; Wideburg, N. E.; Paul, D. A.; Knigge, M. F.; Vasavanonda, S.; et al. *J. Med. Chem.* **1990**, *33*, 2687–2689. Propst, C. L.; Perun, T. J. In *Computer-Aided Drug Design, Methods and Applications*, Perun, T. J., Propst, C. L., Eds.; Marcel Dekker Inc.: New York, 1989; pp 1–19. Bartlett, P. A.; Sampson, N. S.; Reich, S. H.; Drewry, D. H.; Lamden, L. A. In *Use of X-Ray crystallography in the design of Antiviral Agents*; Laver, G., Air, G., Eds.; 1989. Martin, Y. C. In *Crystallographic Modeling Methods in Molecular Design*; Bugg, C. E., Ealick, S. E., Eds.; Springer: New York, 1990; pp 254–263. Baldwin, J. J.; Ponticello, G. S.; Anderson, P. S.; Christy, M. E.; Murcko, M. A.; Randall, W. C.; Schwam, H.; Sugrue, M. F.; Gautheron, P.; et al. *J. Med. Chem.* **1989**, *32*, 2510–2513. Topliss, J. G. *J. Med. Chem.* **1988**, *31*, 2229. Ripka, W. C.; Sipio, W. J.; Blaney, J. M. *Lectures in Heterocyclic Chemistry* **1987**, *IX*, 95–104. Hol, W. G. J. *Pure Appl. Chem.* **1987**, *59*, 431–436. Marshall, G. R. *Ann. Rev. Pharmacol. Toxicol.* **1987**, *27*, 193–213. Pabo, C. O.; Suchanek, E. G. *Biochemistry* **1986**, *25*, 5987–5991. Maag, H.; Locher, R.; Daly, J. J.; Kompis, I. *Helv. Chim. Acta* **1986**, *69*, 887–897. Hansch, C.; Klein, T. E. *Acc. Chem. Res.* **1986**, *19*, 392–400. Freudenreich, C.; Samama, J.-P.; Biellmann, J.-F. *J. Am. Chem. Soc.* **1984**, *106*, 3344–3353. Blaney, J. M.; Jorgensen, E. C.; Connolly, M. L.; Ferrin, T. E.; Langridge, R.; Oatley, S. J.; Burridge, J. M.; Blake, C. C. F. *J. Med. Chem.* **1982**, *25*, 785–790.

0002-7863/94/1516-3251$04.50/0

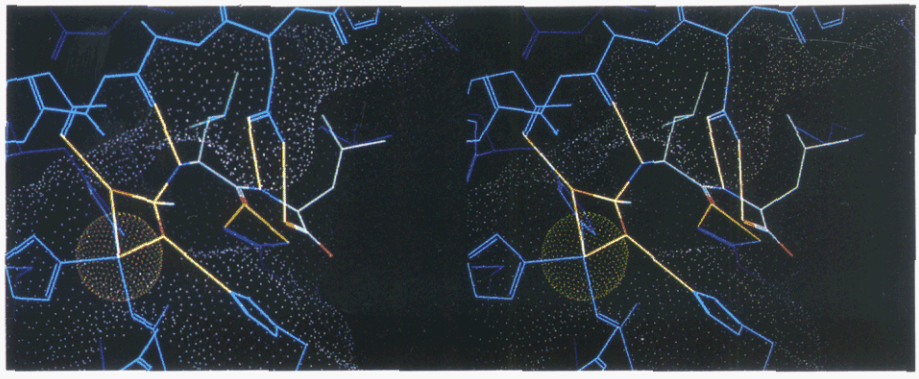

Figure 1. The active site region of the complex of Cbz-Gly^P-Leu-Leu (color-coded) with thermolysin (light blue). The zinc atom is represented by the yellow sphere; hydrogen bonding and other polar interactions to the heteroatoms in the Gly^P-Leu-Leu segment are indicated by yellow lines. The Cbz moiety is truncated by the front clipping plane in this view. The dot surface of the protein represents the solvent-accessible surface according to Connolly.[11]

planned or its effect verified through three-dimensional structural studies.[8]

The complexes between the zinc endopeptidase thermolysin and a series of phosphonate peptide inhibitors presented an unusual chance to probe a number of these questions. Because the structures of these complexes have been determined through X-ray crystallography,[9] they represent systems in which the bound conformation of a flexible peptide analog is known accurately. This system represented an opportunity to evaluate methods for structure-based design and the value of conformational restriction, and it also provided a chance to judge their success through three-dimensional structural studies.

Design of a Cyclic Inhibitor

The complex between thermolysin and Cbz-Gly^P-Leu-Leu (K_i = 9 nM; "Gly^P" represents the phosphonic acid analog of glycine) was chosen as the starting point for design (Figure 1).[10] In the active site, this inhibitor adopts a β-turn-like conformation between the two leucine residues, with the side chains occupying the S_1' and S_2' binding pockets. In addition to this hydrophobic binding, all of the polar atoms in the inhibitor are involved in specific interactions with the enzyme: the anionic phosphorus oxygens are coordinated to the active site zinc cation and to the side chains of Glu-143 and His-231; there are hydrogen bonds from the phosphonamidate NH to the carbonyl oxygen of Ala-113, from the NH of the terminal leucine to the side chain oxygen of Asn-112, to the carbonyl oxygen of the P_1' leucine from the side chain of Arg-203, and to the terminal carboxylate from the side chain NH_2 of Asn-112. These hydrogen bonds not only position the inhibitor in the active site but are also important energetically, since they counteract the effect of desolvating the two components when binding occurs.

In addition to the geometric complementarity that exists between the enzyme and Cbz-Gly^P-Leu-Leu, there are steric constraints in the active site region between the ends of the β-turn. The imidazole of His-231 and the side-chain carboxamide of Asn-112, both of which have key interactions with the inhibitor, are only 6.3 Å apart in the thermolysin/Cbz-Gly^P-Leu-Leu complex. The position of these side chains should presumably not be disrupted, since their polar bonds to the inhibitor appear to be important.[4f,12] Thus, any design that would increase the bulk of the inhibitor in this region must contend with the steric constriction that these residues present.

To constrain this inhibitor so that, throughout the critical region of interaction, it would adopt the conformation observed in the crystal structure, we focused our attention on designing a linking group to connect the carbon α to the phosphorus atom with the terminal carboxylate to form a macrocyclic structure. There were several factors to consider in devising the bridging unit: (1) it should preserve the distance between the Cα carbons of the P_1 and P_2' residues and not introduce any torsional interactions that would perturb the conformation of the inhibitor backbone; (2) it should, itself, be conformationally rigid; (3) it should be accommodated in the narrow entrance to the active site, as described above.

The bridging unit that we devised is the 2(*S*),8-linked chroman as shown in structure (*S*,*S*)-**1** (Figure 2). The anticipated conformation and orientation for this molecule in the thermolysin active site are shown in Figure 3. The bicyclic moiety appeared to satisfy the criteria listed above and also to offer the ether oxygen as a potential hydrogen bond acceptor in place of the carboxylate moiety. The Cbz-NH moiety of Cbz-Gly^P-Leu-Leu was not incorporated in this design since interaction with the S_2 subsite of thermolysin is not necessary for tight binding inhibitors.[13] The aromatic methyl substituent was added to the design

(4) (a) Jencks, W. P. *Adv. Enzymol.* **1975**, *43*, 219–410. (b) Fersht, A. *Enzyme Structure and Mechanism*, 2nd ed.; Freeman: New York. (c) Lemieux, R. U. *Chem. Soc. Rev.* **1989**, *18*, 347–374. (d) Quiocho, F. A. *Pure Appl. Chem.* **1989**, *61*, 1293–1306. (e) Street, I. P.; Rupitz, K.; Withers, S. G. *Biochemistry* **1989**, *28*, 1581–1587. (f) Morgan, B. P.; Scholtz, J. M.; Ballinger, M., Zipkin, I.; Bartlett, P. A. *J. Am. Chem. Soc.* **1991**, *113*, 297–307. (g) Lau, F. T.; Fersht, A. R. *Biochemistry* **1989**, *28*, 301–304.

(5) (a) Lau, F. T.; Fersht, A. R. *Biochemistry* **1989**, *28*, 6841–6847, and references therein. (b) Phillips, M. A.; Kaplan, A. P.; Rutter, W. J.; Bartlett, P. A. *Biochemistry* **1992**, *31*, 959–962.

(6) Cram, D. J. *Angew. Chem., Int. Ed. Engl.* **1986**, *25*, 1039–1057. Page, M. I.; Jencks, W. P. *Proc. Natl. Acad. Sci. U.S.A.* **1971**, *8*, 1678–1683. Benson, S. W.; Cruickshank, F. R.; Golden, D. M.; Haugen, G. R.; O'Neal, H. E.; Rogers, A. S.; Shaw, R.; Walsh, R. *Chem. Rev.* **1969**, *69*, 279.

(7) *Inter alia*: Davies, J. S. *Amino Acids Pept.* **1992**, *23*, 211–48. Hruby, V. J.; Al-Obeidi, F.; Kazmierski, W. *Biochem. J.* **1990**, *268*, 249–262. Struthers, R. S.; Tanaka, G.; Koerber, S. C.; Solmajer, T.; Baniak, E. L.; Gierasch, L. M.; Vale, W.; Rivier, J.; Hagler, A. T. *Proteins: Struct., Funct., Genet.* **1990**, *8*, 295–304. Freidinger, R. M.; Williams, P. D.; Tung, R. D.; Bock, M. G.; Pettibone, D. J.; Clineschmidt, B. V.; DiPardo, R. M.; Erb, J. M.; Garsky, V. M.; Gould, N. P.; Kaufman, M. J.; Lundell, G. F.; Perlow, D. S.; Whitten, W. L.; Veber, D. F. *J. Med. Chem.* **1990**, *33*, 1843–1845. Goodman, M.; Rone, R.; Manesis, N.; Hassan, M.; Mammi, N. *Biopolymers* **1987**, *26*, S25–S32. Hruby, V. J. *Life Sci.* **1982**, *31*, 189–199.

(8) McDowell, R. S.; Gadek, T. R. *J. Am. Chem. Soc.* **1992**, *114*, 9245–9253. Rizo, J.; Koerber, S. C.; Bienstock, R. J.; Rivier, J.; Hagler, A. T.; Gierasch, L. M. *J. Am. Chem. Soc.* **1992**, *114*, 2852–2859. Gurrath, M.; Mueller, G.; Kessler, H.; Aumailley, M.; Timpl, R. *Eur. J. Biochem.* **1992**, *210*, 911–921. Thaisrivongs, S.; Blinn, J. R.; Pals, D. T.; Turner, S. R. *J. Med. Chem.* **1991**, *34*, 1276–1282. Weber, A. E.; Halgren, T. A.; Doyle, J. J.; Lynch, R. J.; Siegl, P. K. S.; Parsons, W. H.; Greenlee, W. J.; Patchett, A. A. *J. Med. Chem.* **1991**, *34*, 2692–2701. Hruby, V. J.; Mosberg, H. I.; Sawyer, T. K.; Knittel, J. J.; Rockway, T. W.; Ormberg, J.; Darman, P.; Chan, W. Y.; Hadley, M. E. *Biopolymers* **1983**, 22, 517–530. Kessler, H. *Angew. Chem.* **1982**, *94*, 509–520.

(9) Matthews, B. W. *Acc. Chem. Res.* **1988**, *21*, 333–340, and references therein.

(10) Tronrud, D. E.; Holden, H. M.; Matthews, B. W. *Science* **1987**, *235*, 571–574.

(11) Connolly, M. L. *J. Appl. Crystallogr.* **1983**, *16*, 548–558. Connolly, M. L. *Science* **1983**, *221*, 709–713.

(12) Phillips, M. A.; Kaplan, A. P.; Rutter, W. J.; Bartlett, P. A. *Biochemistry* **1992**, *31*, 959–962.

(13) Powers, J. C.; Kam, C. M.; Norikaza, N. *Biochemistry* **1979**, *18*, 3032–3038.

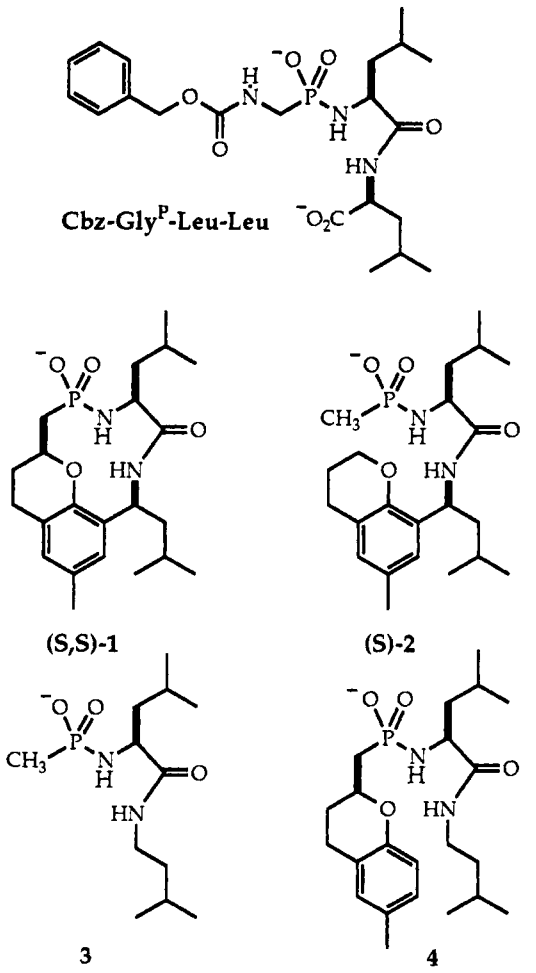

Figure 2. Structures of cyclic inhibitor and acyclic control compounds.

to make it easier to synthesize. No impact on binding was anticipated from this addition, since this region of the bridge was not expected to interact with the enzyme.

Several control compounds were designed to assess the success of our design and to gauge the binding enhancement it produced (Figure 2). The acyclic analogs (*S*)-**2** and **3** were designed to measure the effect of cyclization and to control for the influence of the bridge itself. The simple analogue **3** contains the basic *N*-phosphonyl leucine amide unit without the bicyclic bridge, while (*S*)-**2** differs from **1** by cleavage of the bond β to phosphorus. The latter control was chosen over an alternative structure in which the other linking bond is eliminated (e.g., **4**), since we anticipated that rotation around the P–Cα bond would lead to a different mode of binding, with the chroman moiety in the S_2 pocket of thermolysin.

Synthesis

The synthesis of **1** and its stereoisomers from *p*-cresol is outlined in Scheme 1. The lactone **5** was prepared from Lewis acid-catalyzed addition of *p*-cresol to acrylonitrile according to the published procedure.[14] Treatment with dimethyl lithiomethylphosphonate gives the ketophosphonate **6** in 95% yield as an equilibrium mixture of hemiketal and hydroxyketone isomers. Reduction of this mixture with triethylsilane in the presence of boron trifluoride traps the cyclic form and provides racemic ether **7** in 89% yield.[15] The phenone **8**, formed in 90% yield by Friedel–Crafts acylation of **7** with isovaleryl chloride and titanium tetrachloride, was subjected to a number of procedures for reductive amination. The most efficient proved to be borane reduction of methoxime **9**,[16] followed by protection as the benzyl carbamate **10**; the overall yield is 45–60% from ketone **8**. Attempts to carry out this reductive amination asymmetrically, for example, via borane reduction of the methoxime in the presence of diphenylvalinol,[17] were not successful when performed on the mixture of *syn* and *anti* isomers of methoxime **9**; separation of these isomers proved to be impractical.

At this stage, the two racemic diastereomers can be separated by chromatography and carried on in subsequent reactions in parallel. Partial deprotection of the dimethyl phosphonate is achieved in refluxing *tert*-butylamine;[18] anion and cation exchange provide the sodium salt **11** which is used in the subsequent coupling step. The phosphonate is activated by conversion to the acid chloride with oxalyl chloride and treated with an excess of the free base of L-leucine benzyl ester to give phosphonamidate **12** in 50–70% yield from diester **10**. Two more stereocenters are introduced into the molecule by this coupling reaction, but the resulting diastereomers are not separated until after deprotection and cyclization. Hydrogenolysis of the benzyl protecting groups provides the zwitterionic amine–acids as a mixture of four diastereomers in both cases. The macrocyclization reaction is performed on these mixtures with diphenylphosphoryl azide (DPPA) and $NaHCO_3$ in dimethylformamide under dilute conditions and proceeds in 50–60% yield for the two steps.[19]

From each cyclization mixture only three diastereomers of **13** could be isolated, suggesting that one of the isomers in each case fails to cyclize under the conditions. In both series, the macrocyclic lactam **13** could be partially separated by chromatography into a single, less polar diastereomer and a pair of more polar diastereomers. Preparative separation of the latter pairs of isomers was unnecessary, since in both cases they are converted to the same compound on cleavage of the phosphonate methyl ester. For two of the isomeric fractions of **13**, ester hydrolysis can be accomplished by hydrolysis with lithium hydroxide in acetonitrile; for the other two, demethylation with trimethylsilyl bromide in benzene with pyridine[20] is required. The stages at which the various isomers are separated in this sequence is represented schematically in Figure 4.

This sequence provided pure samples of all of the diastereomers of **1**. The synthetic route dictates that the *R,S*- and *S,R*- isomers are separated from the *R,R*- and *S,S*-isomers at step C (Figure 4) and that chromatography of the cyclic products (step F) separates the *R,S*- from the *S,R*-isomer and likewise the *R,R*- from the *S,S*-. However, which was which could not be inferred from the synthesis; nor were we able to complete the stereochemical assignments by NMR. Although we made tentative assignments on the basis of their binding affinities, the configuration of the *S,S*-isomer was eventually determined by crystallographic analysis of a complex with thermolysin (see below). We do not have a firm basis for assignment of the *R,S*- and *S,R*-isomers.

The simple acyclic control **3** is prepared by phosphonylation of leucine 3-methylbutylamide with methyl methylphosphonochloridate, followed by hydrolysis with lithium hydroxide. Synthesis of the control **2** is outlined in Scheme 2. The methyl-substituted chroman **14** is formed by reduction of lactone **5** and cyclization via the primary bromide.[21] Friedel–Crafts acylation,

(14) Sato, K.; Amakasu, T.; Abe, S. *J. Org. Chem.* **1964**, *29*, 2971.
(15) Kraus, G. A.; Frazier, K. A.; Roth, B. D.; Taschner, M. J.; Neuenschwander, K. *J. Org. Chem.* **1981**, *46*, 2417–2419.
(16) Feuer, H.; Braunstein, D. M. *J. Org. Chem.* **1969**, *34*, 1817–1821.
(17) Itsuno, S.; Sakurai, Y.; Shimizu, K.; Ito, K. *J. Chem. Soc., Perkin Trans. I* **1989**, 1548–1549. Itsuno, S.; Nakano, M.; Miyazaki, K.; Masuda, H.; Ito, K.; Hirao, A.; Nakahama, S. *J. Chem. Soc., Perkin Trans. I* **1985**, 2039–2044. Sakito, Y.; Yoneyoshi, Y.; Suzukamo, G. *Tetrahedron Lett.* **1988**, *29*, 223–224.
(18) Gray, M. D. M.; Smith, D. J. H. *Tetrahedron Lett.* **1980**, *21*, 859–862.
(19) Brady, S. F.; Freidinger, R. M.; Paleveda, W. J.; Colton, C. D.; Homnick, C. F.; Whitten, W. L.; Curley, P.; Nutt, R. F.; Veber, D. F. *J. Org. Chem.* **1987**, *57*, 764–769. Ewing, W. R.; Harris, B. D.; Li, W.-R.; Jouillé, M. M. *Tetrahedron Lett.* **1989**, *30*, 3757–3760.
(20) McKenna, C. E.; Higa, M. T.; Cheung, N. H.; McKenna, M.-E. *Tetrahedron Lett.* **1977**, 155–158. McKenna, C. E.; Schmidhauser, J. *J. Chem. Soc., Chem. Commun.* **1979**, 739.

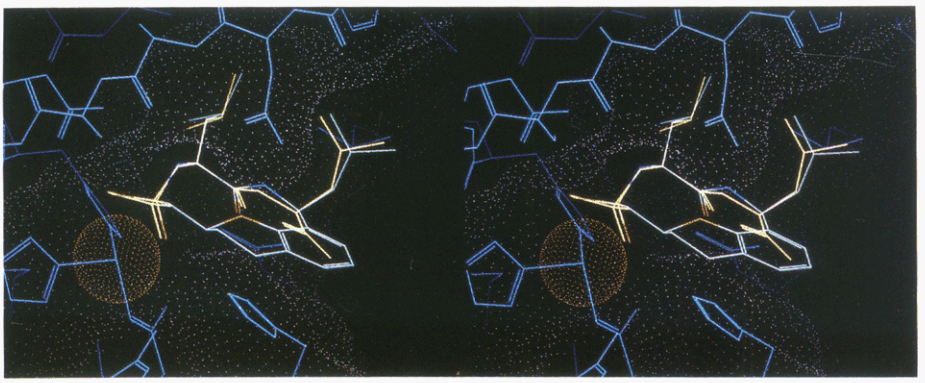

Figure 3. Superposition of the modeled orientation of (*S*,*S*)-**1** (atoms color coded) and the experimental structure of Cbz-Gly^{P}-Leu-Leu (yellow) in the active site of thermolysin.

Scheme 1

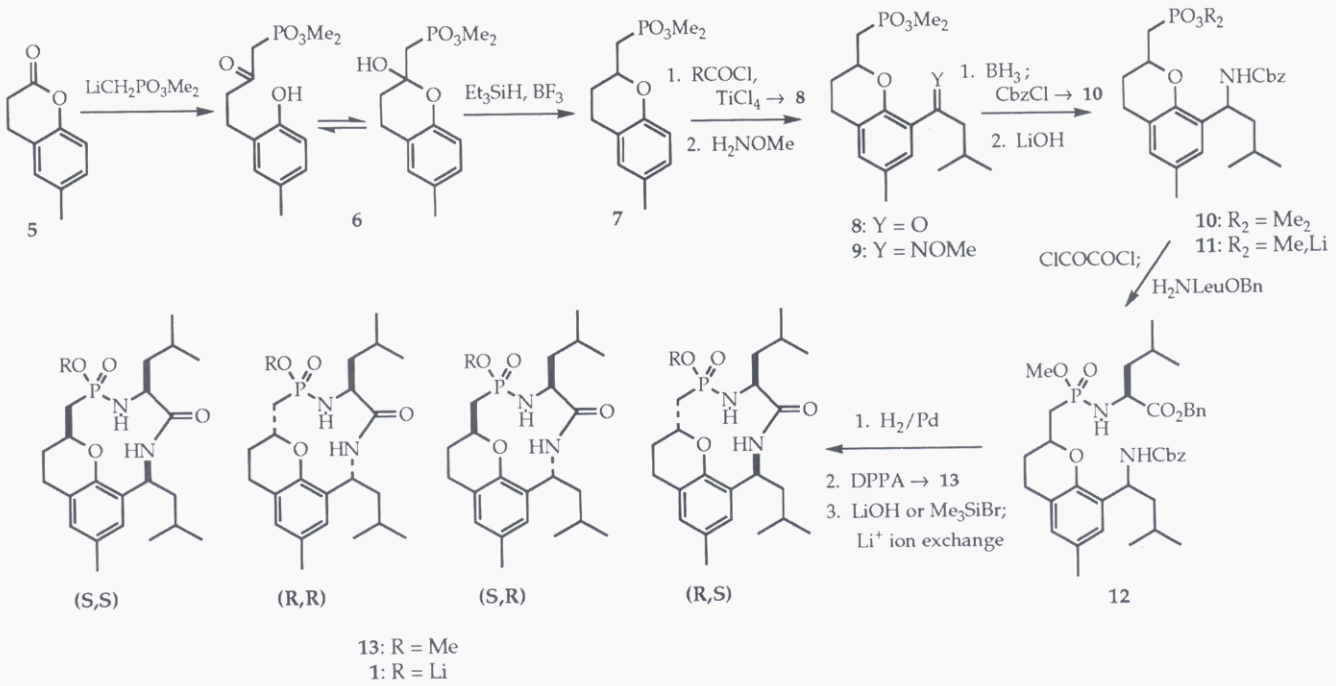

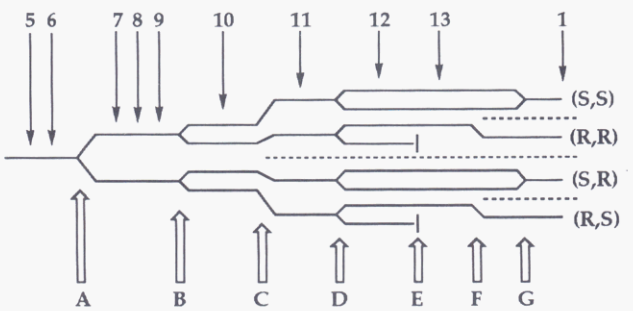

Figure 4. Schematic representation of the synthesis of **1**, showing steps in which stereocenters are formed or removed or diastereomers are separated. Each line represents a single stereoisomer; compound numbers are shown across the top: A and B, introduction of first and second stereocenters; C, separation of diastereomers of **10**; D, generation of stereocenter at phosphorus; E, cyclization and loss of two diastereomers; F, separation of diastereomers of macrocycle **13**; G, loss of stereocenter at phosphorus on hydrolysis.

formation of the methoximes **16**, reduction to the racemic amine, and coupling with *N*-Cbz-leucine to give **17** parallels the route used for preparation of the macrocyclic analogs. The diastereomers of **17** can be separated on reverse-phase HPLC. Deprotection, phosphonylation, and hydrolysis of the separate diastereomers of **18** then complete the synthesis of the controls (*R*)-**2** and (*S*)-**2**.

The diastereomers of **17** were tentatively assigned as (*R*)-**17** ($[\alpha]_D$ (MeOH) +24.7°) and (*S*)-**17** ($[\alpha]_D$ (MeOH) –33.7°) by chiroptical comparison to the authentic diastereomers of *N*-(Cbz)-leucine 1-phenylethylamide: ((*R*)-**19**: $[\alpha]_D$ (MeOH) + 1.2°, and (*S*)-**19**: $[\alpha]_D$ (MeOH) –16.4°). Supporting evidence was obtained by asymmetric reduction of the *E*-oxime of **16** with the borane/(*S*)-diphenylvalinol complex, which forms the *S*-isomer selectively in related systems.[17] With this reagent, a 70% diastereomeric excess of the (*S*)-leucinamide (*S*)-**17** is obtained after acylation.

Finally, the crystal structure of the complex between thermolysin and (*S*)-**2** provided unambiguous evidence for this assignment.

Enzymatic Evaluation

The inhibition constants of the various stereoisomers of **1**, **2**, and **3** were determined at pH 7.0 at 25 °C under standard conditions[22] (Table 1). The macrocyclic analogue (*S*,*S*)-**1** is a potent inhibitor of thermolysin, with a K_i value of 4 nM at pH 7.5. Comparison of this value with the inhibition constants for

(21) Bradsher, C. K.; Reames, D. C. *J. Org. Chem.* **1981**, *46*, 1384–1388. Hirsch, J. A.; Schwartzkopf, G. *J. Org. Chem.* **1973**, *38*, 3534–3536. Houry, S.; Garesh, S.; Shani, A. *Isr. J. Chem.* **1973**, *11*, 805–817.

(22) Bartlett, P. A.; Marlowe, C. K. *Biochemistry* **1983**, *22*, 4618–4624.

Scheme 2

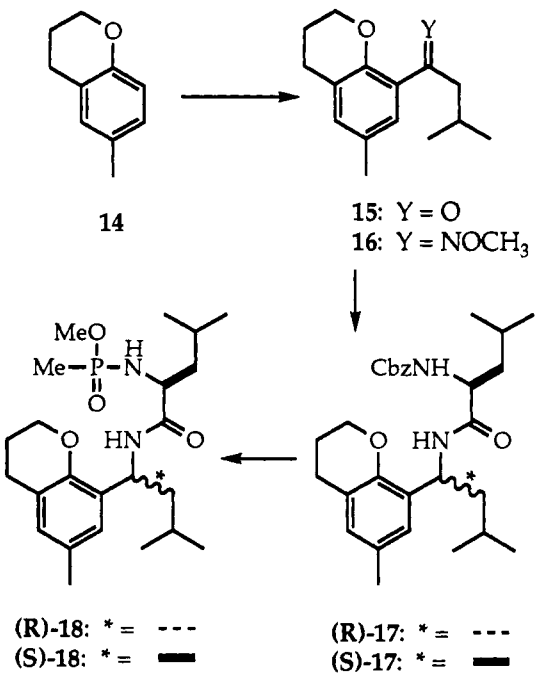

Table 1. Inhibition of Thermolysin by Cyclic and Acyclic Phosphonamidates[a]

compound	K_i (nM)	compound	K_i (nM)
(*S,S*)-**1**	4	(**R**)-**2**	1900
(*S*)-**2**	80	(**R,S**)-**1**[b]	>10000
3	190	(**R,R**)-**1**	>10000
(*S,R*)-**1**[b]	500		

[a] Determined at 25 °C, pH 7.5, as described in ref 21. [b] Tentative stereochemical assignment.

Table 2. Data Collection and Refinement Statistics

	inhibitor complex	
	(S,S-1)	(S)-2
Data Collection		
resolution (Å)	1.65	1.80
no. of independent reflcns	33083	26699
completeness of data (%)	86.6	85.1
R_{merge} (%)[a]	7.0	3.8
av isomorphous difference (%)	13.0	12.6
Refinement		
resolution	1.70	1.82
reflctns included	32986	26548
residual (%)	16.8	17.0
Δ_{bonds} (Å)	0.015	0.017
Δ_{angles} (deg)	2.2	2.3

[a] R_{merge} gives the average agreement between independently measured intensities; the average isomorphous difference gives the average difference between the measured structure amplitudes of the inhibitor complex and that of the native crystals; Δ_{bonds} and Δ_{angles} give the average discrepancies between the bond lengths and angles in the final refined model and the values expected for "ideal" stereochemistry.

the stereoisomers of **1** and for the various control compounds (Table 1) indicates that incorporation of the correct bridging unit leads to a significant enhancement in binding affinity. The most potent isomer of **1** was presumed to be the desired (*S,S*)-diastereomer, an assignment that was confirmed by the crystallographic studies described below. The synthetic scheme dictates that the isomer of modest affinity (k_i = 500 nM) differs from (*S,S*)-**1** at one stereocenter, either having the opposite configuration β to the phosphorus or at the benzylic position. The 125-fold difference in affinity is comparable to that shown by thermolysin for L- versus D-configured amino acids at the P_2' position[23] (and compare (*S*)- and (*R*)-**2**), hence we have provisionally assigned

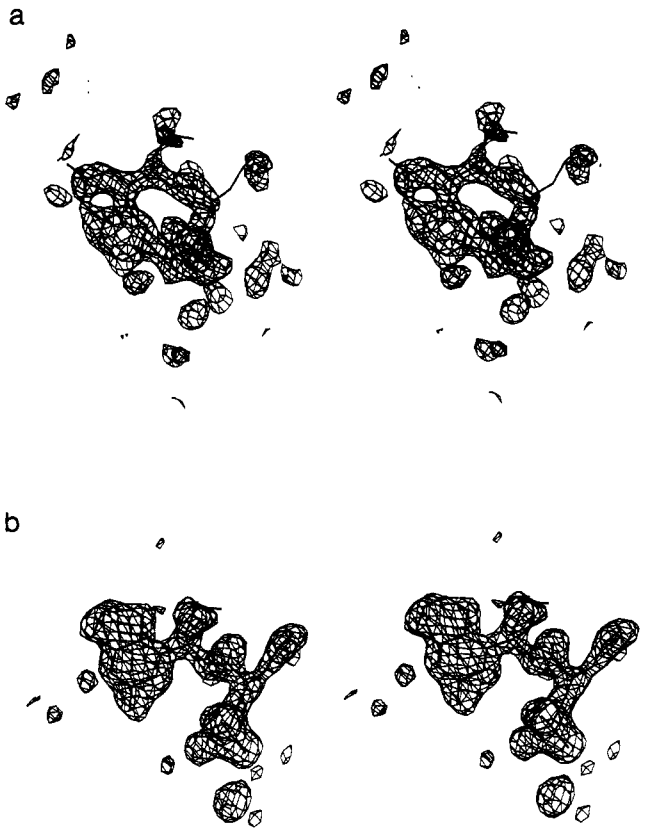

Figure 5. Initial map showing the electron density corresponding to the bound inhibitors. Coefficients (F_{PI}–F_C) where F_{PI} is the observed structure amplitude of the protein-inhibitor complex and F_C is the amplitude calculated from the refined model of thermolysin[25] with solvent molecules removed from the active site region. Phases, ϕ_c, correspond to the amplitudes F_C. Map contoured at 3.0σ where σ is the root-mean-square density throughout the unit cell. Refined inhibitor model is superimposed: (a, top) inhibitor (*S,S*)-**1**. (b, bottom) inhibitor (*S*)-**2**.

the (*S,R*)-configuration to the 500-nM inhibitor. However, we cannot rule out the possibility that this inhibitor has the (*R,S*)-configuration. The remaining two isomers of **1** show little inhibition, even at concentrations above 10 μM, indicating that the stereoisomers with the (*R*)-configuration at the chroman linkage must adopt a relatively high-energy conformation if they are to fit into the active site at all.

Although we anticipated that these inhibitors could be slow-binding, in view of their reduced flexibility, the kinetic assays gave no evidence of the cyclic analogues binding more slowly to thermolysin than is observed for typical substituted phosphonate peptide derivatives.[24]

Structural Evaluation

Crystallographic analysis of the complexes of the macrocycle (*S,S*)-**1** and the acyclic control (*S*)-**2** confirmed the tentative stereochemical assignments described above (Figures 5–7). In addition, (*S,S*)-**1** can be compared in its binding with (*S*)-**2**, with the original inhibitor Cbz-Gly^P-Leu-Leu, and with the original model design. For the most part, the common components of these inhibitors adopt nearly identical orientations within the thermolysin active site (Figures 6 and 7); however, there are some important differences.

From the Cα-carbon of the phosphonate residue to the Cα-carbon of the P_2' moiety, the backbone and side-chain atoms of the three inhibitors adopt similar orientations in the active site and engage in similar polar and steric contacts with the protein.

(23) Morihara, K.; Tsuzuki, H. *Eur. J. Biochem.* **1970**, *15*, 374–380.
(24) Bartlett, P. A.; Marlowe, C. K. *Biochemistry*, **1987**, *26*, 8553–8561. Izquierdo-Martin, M.; Stein, R. L. *J. Am. Chem. Soc.* **1992**, *114*, 1527–1528.

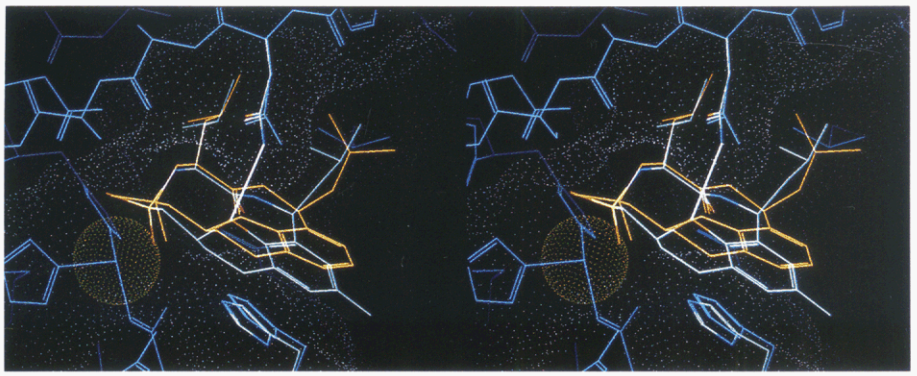

Figure 6. Comparison of modeled (orange) and observed (color-coded) conformations of (*S*,*S*)-**1** in active site of thermolysin (blue) (the *p*-methyl substituent is absent in modeled structure). The protein structure is taken from the complex with Cbz-Gly^{P}-Leu-Leu; color-coded representations of the side-chains of His-231 and Asn-112 (above and below the inhibitor, respectively) indicate the different orientations they adopt in the (*S*,*S*)-**1** complex.

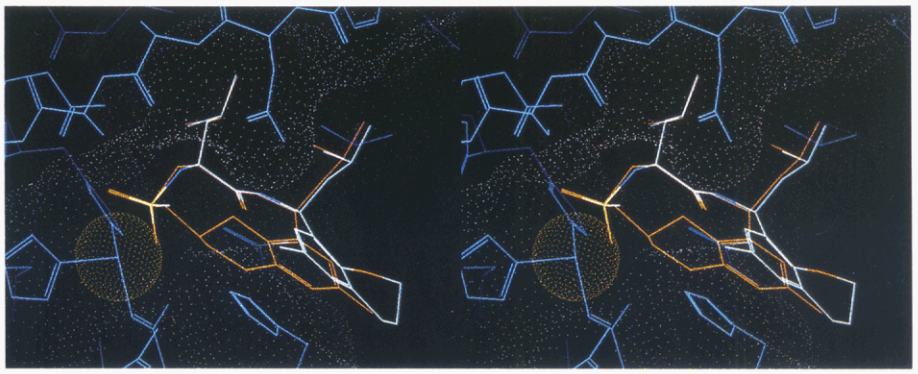

Figure 7. Comparison of bound conformations of cyclic inhibitor (*S*,*S*)-**1** (red) and acyclic control (*S*)-**2** (color-coded).

In comparison to the original modeled structure for the macrocyclic inhibitor, the plane of the bridging chroman unit in (*S*,*S*)-**1** is rotated by 12°, which brings it closer and more parallel to the imidazole of His-231. This displacement is accommodated in part by a 0.4-Å movement of the His-231 side chain itself, relative to its position in the Cbz-Gly^{P}-Leu-Leu complex, which leads to a wider opening to the active site. The different orientation of the chroman unit corresponds to a rotation of 17° about the NH-to-Cα bond of the pseudo P_2' residue, forcing the appended isobutyl group closer to the Asn-112 carboxamide. To reduce this steric interaction, a different conformation is adopted by the isobutyl side chain, involving a rotation of 138° about the Cα to Cβ bond and 163° about the Cβ–Cγ bond. This distortion indicates that the chroman unit is not perfect in its ability to bridge the ends of the inhibitor without clashing with the enzyme. Our original modeling efforts would not have uncovered the different binding orientation, since alternative energy minima were not explored at that time.

One of the consequences of replacing the terminal carboxylate group of Cbz-Gly^{P}-Leu-Leu with the neutral chroman unit in **1** is disruption of the hydrogen bond between the carboxylate moiety and the side-chain amide of Asn-112. In the complex with (*S*,*S*)-**1**, the protein accommodates this structural change by a 24° rotation of the Asn side chain about the Cβ–Cγ bond, enabling the carboxamide to donate a hydrogen bond to the ether oxygen of the bridge (N–O distance of 3.1 Å), while continuing to accept a hydrogen bond from the inhibitor amide nitrogen. The orientation of this amide linkage suggests that it provides a bifurcated hydrogen bond to the Asn-112 side chain (N–O distance of 3.3 Å) and transannularly to the ether oxygen (N–O distance of 2.6 Å).

Determination of the bound conformation of the acyclic control (*S*)-**2** shows that backbone and side-chain atoms of this analogue are virtually superimposable with the corresponding atoms in the complex with the macrocyclic inhibitor (*S*,*S*)-**1** (rms deviation 0.25 Å). However, the chroman unit of (*S*)-**2** is rotated 168° in comparison with that in (*S*,*S*)-**1** (Figure 6). In contrast with (*S*,*S*)-**1**, the distal part of the chroman unit in (*S*)-**2** is exposed to solvent and makes no contacts either with the rest of the inhibitor or with the thermolysin molecule. The chroman oxygen forfeits an intramolecular hydrogen bond with the backbone nitrogen of the inhibitor but does hydrogen bond to a locally ordered solvent molecule.

Chemically, the acyclic control differs from the macrocycle only by the addition of two hydrogens in place of a carbon–carbon bond. However, from a structural point of view, this alteration requires that the carbon–carbon distance increase from the covalent bond length of 1.5 Å to the van der Waals contact distance of CH groups, i.e., about 3.8 Å. Apparently, there is not enough leeway in the thermolysin active site, particularly in the region between Asn-112 and His-231, to accommodate this increase in distance without the observed reorientation of the chroman moiety.

Appraisal of the Approach

Incorporation of the chroman moiety in the macrocyclic phosphonamidate (*S*,*S*)-**1** results in a 50-fold increase in affinity for thermolysin in comparison with the basic inhibitor **3**. This increase comes both from the inherent affinity of the chroman unit itself and from its constraint of the peptide chain. The acyclic control (*S*)-**2** was designed to distinguish the respective contributions from these two factors. However, the bicyclic moiety in (*S*)-**2** adopts a different position in the active site ("exo") than the macrocycle (*S*,*S*)-**1**, which means that the 20-fold difference in affinity between these two molecules is not simply the result of cyclization. The differential binding affinity of the chroman unit versus hydrogen may be larger or smaller than the observed difference of 0.5 kcal/mol between **3** and (*S*)-**2**. Although it is tempting to suggest that a hydrogen bond between the ether oxygen and Asn-112 would favor an "endo"orientation of the chroman unit (in the absence of steric interference with a phosphorus–

carbon substituent), it is possible that steric interference from the active site would offset this favorable effect.

The diastereomeric macrocycle (*R,S*)-**1**, with a K_i value more than three orders of magnitude higher than that for **3**, demonstrates the penalty exacted for incorrect constraint. Although this structure can be modeled into the active site of thermolysin without significant steric interactions with the protein, it must adopt a high-energy conformation with an eclipsed relationship between the adjacent C–P and C–O bonds.

No direct evidence for the conformation of (*S,S*)-**1** in solution was obtained from the NMR spectrum, since NOE interactions could not be observed between the nonexchangeable spin systems of the left and right halves of the molecule. However, the carboxamide hydrogen of (*S,S*)-**1** is slow to exchange in CD_3OD, suggesting that this molecule adopts an internally hydrogen-bonded conformation in solution like that in the active site, where the amide N–H donates a bifurcated hydrogen bond to the ether oxygen and Asn-112. Similar slow exchange is seen for the acyclic control (*S*)-**2**, but not **3**.[26]

Structure-based design approaches, whether they involve *de novo* design, design of a mimic, or conformational restriction of a known ligand, have generally pursued complementarity between the static structures of ligand and binding site, i.e., the "lock and key" model.[27] However, even in their complex, the ligand and the receptor are not rigid.[28] Residual thermal motion in the complex tends to reduce the enthalpy of binding as the atoms involved in various polar and van der Waals interactions move from their equilibrium positions; however, the entropy associated with this residual motion is favorable, and to inhibit it would tend to reduce the free energy of binding. Thus, optimizing the design of a conformationally constrained ligand presents a dilemma. Should the unbound ligand be rigidified only to the extent that it is confined in the complex, in order to allow for similar residual motion? Or should it be made as inflexible as possible, in order to optimize the enthalpic interactions with the binding site? It is conceivable that a mismatch in the dynamical characteristics of ligand and receptor could limit receptor motion,[29] leading to the seemingly incongruous result that over-rigidification of the inhibitor may lead to an unfavorable rather than a favorable contribution to the entropy of binding. The importance to binding affinity of *dynamical complementarity* between ligand and receptor has, to our knowledge, not yet been addressed, either experimentally or computationally, but it may prove to be an important consideration in structure-based design.

A separate but related issue is that of slow-binding behavior.[30] While slow-binding is often attributed to slow interconversion of protein conformational states, it may also arise if the normal pathway for association requires a number of ligand conformations not available to a constrained inhibitor.[31] However, while phosphonamidates and related analogues are generally slow-binding inhibitors of thermolysin,[24] it is interesting to note that the macrocyclic inhibitor (*S,S*)-**1** is not unusual in this respect.

A close coupling of binding studies and structure determination will become increasingly important for the advancement of structure-based design of enzyme inhibitors and ligands for other macromolecular receptors. Binding studies require appropriate control or comparison compounds to provide insight into the basis of the observed affinity. However, the interpretation of these binding effects remains speculative without structural characterization of the protein–ligand complexes themselves. Furthermore, structural information provides a necessary foundation for further design enhancements. The successful design of the macrocyclic thermolysin inhibitor demonstrates the power of this combined approach.

Experimental Section[32]

Modeling Studies. The inhibitor (*S,S*)-**1** was designed before we had very much experience with or access to molecular modeling systems. Dreiding models, MM2 calculations (improperly parametrized for phosphonates) on a PC, and stereo slides taken with the assistance of the Computer Graphics Laboratory using the Midas program[33] at the University of California, San Francisco, were all used to enhance (rationalize?) our intuition. Additional modeling was performed with PSSHOW (Dearing, A. MOGLI Version 2.2, Evans and Sutherland Corporation) and MacroModel[34] Versions 2.0 and 2.5 (Still, W. C., et al., Columbia University) on an Evans and Sutherland PS350 graphics system. More recent modeling efforts were performed on a Silicon Graphics 4D-70 workstation using MacroModel Version 3.0 and BioGraf Version 2.0 (Molecular Simulations, Inc.), implementing the Dreiding force field.[35] The inhibitor (*S,S*)-**1** was constructed from the enzyme-bound conformation of Cbz-Gly^P-Leu-Leu (5TMN in the Protein Databank[36]) and minimized in the active site. During the minimization, the phosphonate oxygens of the inhibitor were constrained to the respective distances observed in the Cbz-Gly^P-Leu-Leu complex, and the protein was kept rigid. The result of this minimization is shown in Figure 6.

Synthesis of Cyclic Inhibitors. [2*R*-(2*R,6*S**,9*R**)]-3,4,5,6,8,9-Hexahydro-4-hydroxy-11-methyl-6,9-bis(2-methylpropyl)-2,13-ethano-1,5,8,4-benzoxadiazaphosphacycloundecin-7(2*H*)-one-4-oxide, Monolithium Salt, (*R,R*)-1.** A solution of 2.5 mg (0.006 mmol) of (*R,R*)-**13** in 200 μL of CH_3CN with 30 μL of 1 N LiOH was stirred for 48 h. The reaction mixture was concentrated to a white solid which was purified by anion exchange chromatography over Sephadex DEAE with a linear gradient from 1:1 MeOH/H_2O to 1:1 MeOH/1 M TBK buffer, followed by cation exchange chromatography (Dowex in MeOH, Li^+ form). Concentration from CH_3OH resulted in 2.5 mg (100%) of (*R,R*)-**1** as

(25) Holmes, M. A.; Matthews, B. W. *J. Mol. Biol.* **1982**, *160*, 623–629.

(26) 2D NOESY spectra (Bodenhausen, G.; Kogler, K.; Ernst, R. R. *J. Magn. Reson.* **1984**, *58*, 370) of the diastereomeric intermediates **10**, obtained in $CDCl_3$ solution in the course of trying to assign their configurations, showed an NOE interaction between the carbamate hydrogen and the hydrogen α to the ether in both diastereomers, which is also consistent with an internally hydrogen bonded structure.

(27) Fischer, E. *Chem. Ber.* **1894**, *27*, 2985–2993.

(28) Ringe, D.; Petsko, G. A. *Prog. Biophys. Molec. Biol.* **1985**, *45*, 197–235. Roberts, G. C. K. In *Host–Guest Molecular Interactions: From Chemistry to Biology*; Chadwick, D. J., Widdows, K., Eds.; John Wiley & Sons: New York, 1991; pp 169–182.

(29) See, for example: Somogyi, B.; Matko, J.; Rosenberg, A. *Acta Biochim. Biophys. Hung.* **1988**, *23*, 135–148. Cross, A. J.; Fleming, G. R. *Biophys. J.* **1986**, *50*, 507–512. Maliwal, B. P.; Lakowicz, J. R. *Biophys. Chem.* **1984**, *19*, 337–344. James, M. N. G.; Sielecki, A.; Salituro, F.; Rich, D. H.; Hofmann, T. *Proc. Natl. Acad. Sci. U.S.A.* **1982**, *79*, 6137–6141.

(30) Schloss, J. V. *Acct. Chem. Research* **1988**, *21*, 348–353. Morrison, J. F.; Walsh, C. T. *Adv. Enzymol. Relat. Areas Mol. Biol.* **1987**, *61*, 201–301.

(31) Mao, B. *Biochem. J.* **1992**, *288*, 109–116. Burgen, A. S. V.; Roberts, G. C. K.; Feeney, J. *Nature* **1975**, *253*, 753–755.

(32) The following abbreviations are used: triethylammonium bicarbonate (TBK), 1-hydroxybenzotriazole hydrate (HOBT), ethyl dimethylaminoethylcarbodiimide (EDC), and diisopropylethylamine (DIEA). Unless otherwise noted, materials were used as obtained from commercial suppliers. Methylene chloride, acetonitrile, and *tert*-butylamine were dried by distillation from CaH_2 under N_2, tetrahydrofuran (THF) was freshly distilled from sodium/benzophenone under N_2, and dimethylformamide was distilled from calcium oxide at 35 mmHg vacuum and stored over 3Å molecular sieves. TBK buffer was prepared by bubbling CO_2 gas through an aqueous solution of triethylamine until the desired pH was attained. ^1H NMR spectra are presented as follows: chemical shift on the δ scale (multiplicity, number of hydrogens, coupling constant(s) in hertz). ^1H NMR spectra measured in CD_3OD or D_2O are referenced to methanol as 3.30 ppm; ^{13}C NMR spectra are referenced to $CDCl_3$ (77.0 ppm) or CD_3OD (49.0 ppm); ^{31}P NMR spectra are reported downfield from trimethyl phosphate as 3.086 ppm. IR spectra were obtained on neat films unless otherwise indicated. Spectral and analytical characterization obtained for the synthetic intermediates are indicated at the end of each experimental description; full details are provided in the supplementary material.

(33) Ferrin, T. E.; Huang, C. C.; Jarvis, L. E.; Langridge, R. *J. Mol. Graphics* **1988**, *6*, 13–37.

(34) Mohomadi, F.; Richards, N. G. J.; Guida, W. C.; Liskamp, R.; Lipton, M.; Caufield, C.; Chang, G.; Hendrickson, T.; Still, W. C. *J. Comput. Chem.* **1990**, *4*, 440–467.

(35) Mayo, S. L.; Olafson, B. D.; Goddard, W. A., III *J. Phys. Chem.* **1990**, *94*, 8897–8909.

(36) Bernstein, F. L.; Koetzle, T. F.; Williams, G. J. B.; Meyer, E. F., Jr.; Brice, M. D.; Rodgers, J. R.; Kennard, O.; Shimanouchi, T.; Tasumi, M. *J. Mol. Biol.* **1977**, *185*, 535–542.

(37) Henderson, P. J. F. *Biochem. J.* **1972**, *127*, 321–333.

(38) Weaver, L. H.; Kester, W. R.; Matthews, B. W. *J. Mol. Biol.* **1987**, *114*, 119–132.

(39) Xuong, N. H.; Nielsen, C.; Hamlin, R.; Anderson, D. *J. Appl. Cryst.* **1985**, *181*, 342–350.

(40) Tronrud, D. E.; Ten Eyck, L. F.; Matthews, B. W. *Acta Crystallogr.* **1987**, *A43*, 489–503. Tronrud, D. E. *Acta Crystallogr.* **1992**, *A48*, 912–916.

a white solid: IR (5% MeOH/$CHCl_3$) 3340, 2960, 1655, 1450, 1423, 1325, 1042 cm^{-1}; ^1H NMR (400 MHz, CD_3OD) δ [0.908 (d, J = 6.5) and 0.916 (d, J = 6.5), 6H], 1.00 (d, J = 6.2) and 1.02 (d, J = 6.2), 6H], 1.28–1.35 (m, 3), 1.39–1.47 (m, 1), 1.53–1.92 (m, 5), 1.98–2.08 (m, 1), 2.22 (s, 3), 2.67–2.88 (m, 2), 3.43–3.50 (m, 1), 3.60–3.66 (m, 1), 4.29–4.50 (m, 1), 6.77 (s, 1), 6.85 (s, 1); ^{31}P NMR (123 MHz, CD_3OD) δ 20.47; MS (FAB) m/z 429 $(MH)^+$; HRMS (FAB) calcd for $LiC_{22}H_{34}N_2O_4P$, 429.2495, found, 429.2501.

[2*R*-(2*R,6*S**,9*S**)]-3,4,5,6,8,9-Hexahydro-4-hydroxy-11-methyl-6,9-bis(2-methylpropyl)-2,13-ethano-1,5,8,4-benzoxadiazaphosphacycloundecin-7(2*H*)-one-4-oxide, Monolithium Salt, (*R*,*S*)-1.** As described above for the (*R*,*R*)-isomer, 8.9 mg (0.02 mmol) of (*R*,*S*)-**13** was converted to 4.7 mg (54%) of (*R*,*S*)-**1** as a white solid: IR (5% MeOH/$CHCl_3$) 3300, 2960, 1650, 1478, 1430, 1045 cm^{-1}; ^1H NMR (400 MHz, CD_3OD) δ [0.925 (d, J = 6.5), 0.946 (d, J = 5.0), 0.951 (d, J = 5.0), and 0.976 (d, J = 6.3), 12H], 1.28–1.67 (m, 6), 1.73–1.84 (m, 2), 1.88–1.95 (m, 1), 2.13–2.20 (m) and 1.95 (s, 4), 2.67 (dd, 1, J = 5.8, 17.0), 2.73–2.81 (m, 1), 3.49–3.63 (m, 2), 4.67–4.73 (m, 1), 6.74 (s, 2), 9.19 (d, 1, J = 10.1); ^{31}P NMR (123 MHz, CD_3OD) δ 21.82; UV 287 nm (ϵ 2350); MS (FAB) m/z 429 $(MH)^+$; HRMS (FAB) calcd for $LiC_{22}H_{34}N_2O_4P$, 429.2495, found, 429.2505. Anal. Calcd for $LiC_{22}H_{34}N_2O_4P$: P, 7.23. Found: P, 4.63 (64% of the solid is inhibitor).

[2*S*-(2*R,6*R**,9*R**)]-3,4,5,6,8,9-Hexahydro-4-hydroxy-11-methyl-6,9-bis(2-methylpropyl)-2,13-ethano-1,5,8,4-benzoxadiazaphosphacycloundecin-7(2*H*)-one-4-oxide, Monolithium Salt, (*S*,*S*)-1.** To a solution of 3 mL of benzene, saturated with isobutylene gas at 12 °C, was added 1.4 mL of pyridine and 320 μL of trimethylsilyl bromide. A solution of 35 mg (0.09 mmol) of (*S*,*S*)-**13** in 2 mL of 1:1 CH_2Cl_2/benzene was added, and the solution was stirred at 12 °C for 1 h and then warmed to room temperature for an additional hour. The reaction mixture was frozen and lyophilized to a white solid. This solid was dissolved in MeOH, filtered though a Dowex cation exchange column (MeOH, Li^+ form) to remove the pyridinium salts, and then concentrated to a white solid. After dissolution in water, the salt was purified by anion exchange chromatography over Sephadex DEAE with a linear gradient from 1:1 MeOH/H_2O to 1:1 MeOH/1 M TBK buffer, followed by cation exchange chromatography (Dowex in MeOH, Li^+ form). Concentration from CH_3OH provided 28.6 mg (83%) of (*S*,*S*)-**1** as a white solid: ^1H NMR (400 MHz, CD_3OD) δ [0.941 (d, J = 6.5) and 0.947 (d, J = 6.6), 9H], 0.997 (d, 3, J = 6.5), 1.37–1.45 (m, 2), 1.65–1.76 (m, 3), 1.80–2.12 (m, 5), 2.19 (s, 3), 2.74 (dd, 1, J = 5.5, 16.7), 2.83–2.92 (m, 1), 3.89 (dt, 1, J = 3.3, 10.6), 4.09 (dd, 1, J = 10.4, 21.2), 4.76–4.82 (m, 1), 6.67 (s, 1), 6.73 (s, 1), 8.97 (d, 1, J = 10.0); ^{13}C NMR (102 MHz, CD_3OD) δ 20.65, 22.08, 22.10, 23.67, 24.01, 25.55, 25.94, 26.01, 31.35 (d, J = 15.7), 38.85 (d, J = 131), 45.09, 47.62, 52.70, 56.90 (d, J = 10.2), 75.50 (d, J = 5.6), 125.03, 127.89, 129.61, 130.43, 130.86, 152.87, 177.93 (d, J = 4.5); ^{31}P NMR (123 MHz, CD_3OD) δ 20.47; MS (FAB) m/z 429 $(MH)^+$; HRMS (FAB) calcd for $LiC_{22}H_{34}N_2O_4P$, 429.2495; found, 429.2495.

[2*S*-(2*R,6*R**,9*S**)]-3,4,5,6,8,9-Hexahydro-4-hydroxy-11-methyl-6,9-bis(2-methylpropyl)-2,13-ethano-1,5,8,4-benzoxadiazaphosphacycloundecin-7(2*H*)-one-4-oxide, Monolithium Salt, (*S*,*R*)-1.** As described above for the (*S*,*S*)-isomer, 10 mg (0.026 mmol) of (*S*,*R*)-**13** was converted to 9.4 mg (84%) of (*S*,*R*)-**1** as a white solid: IR (5% MeOH/$CHCl_3$) 3300, 2960, 1650, 1470, 1450, 1175, 1045 cm^{-1}; ^1H NMR (400 MHz, CD_3OD) δ [0.918 (d, J = 6.7), 0.929 (d, J = 6.6), 0.936 (d, J = 7.3), and 0.972 (d, J = 6.6), 12H], 1.30–1.53 (m, 4), 1.65–1.88 (m, 4), 1.96–2.13 (m, 2), 2.18 (s, 3), 2.63–2.75 (m, 2), 3.80 (dd, 1, J = 7.6, 16.9), 4.64 (dd, 1, J = 5.5, 9.9), 4.76 (t, 1, J = 11.2), 6.71 (s, 1), 6.76 (s, 1); ^{31}P NMR (123 MHz, CD_3OD) δ 20.44; MS (FAB) m/z 429 $(MH)^+$; HRMS (FAB) calcd for $LiC_{22}H_{34}N_2O_4P$, 429.2495, found, 429.2502.

***N*-[1*S*-[[1*S*-(3,4-Dihydro-6-methyl-2*H*-1-benzopyran-8-yl)-3-methylbutyl]amino]carbonyl]-3-methylbutyl]-*P*-methylphosphonamidic Acid, Lithium Salt, (*S*)-2, the Diastereomer (*R*)-2, and *N*-[Methyl(oxy)-phosphinyl]-L-leucine 3-Methylbutylamide, Lithium Salt, 3.** Synthesis and characterization of these control compounds are described in the supplementary material.

2-[4-Dimethoxyphosphinyl)-3-oxobutyl]-4-methylphenol, 6. Dimethyl methylphosphonate (2.52 mmol) was added to a stirring solution of 2.54 mmol of lithium diisopropylamide in 25 mL of THF at –78 °C, under a nitrogen atmosphere, and the reaction mixture was stirred for 2 h; the formation of a white precipitate was observed. A solution of 1.23 mmol of 4-methyldihydrocoumarin, **5**,[14] in 3 mL of THF was added dropwise to the reaction mixture, while the temperature was kept at –78 °C. The mixture was stirred at –78 °C for 4 h, warmed to room temperature, and stirred an additional 12 h. The reaction mixture was treated with 0.5 mL of saturated NH_4Cl and evaporated to dryness, and the residue was dissolved in 10 mL of H_2O and extracted with EtOAc (3 × 25 mL). The combined organic layers were washed with saturated NaCl, dried ($MgSO_4$), and concentrated to yield a yellow oil. Flash chromatography (80% EtOAc/hexane) over silica yielded 327 mg (93%) of **6** as a colorless oil: IR, ^1H NMR; ^{31}P NMR; MS (FAB); Anal.

3,4-Dihydro-2-[(dimethoxyphosphinyl)methyl]-6-methyl-2*H*-1-benzopyran, 7. To a stirring solution of 200 mg of **6** (1.05 mmol) and 1.34 mL of triethylsilane (8.40 mmol) in 53 mL of CH_2Cl_2 at –78 °C, under a nitrogen atmosphere, was added 0.78 mL of BF_3·OEt (6.32 mmol). The solution was stirred at –78 °C for 1 h, warmed to room temperature, and stirred an additional 12 h. The reaction mixture was treated with saturated $NaHCO_3$ (0.5 mL) and diluted with 200 mL of CH_2Cl_2. The organic layer was washed with saturated $NaHCO_3$, dried ($MgSO_4$), and concentrated to yield a yellow oil. Flash chromatography (80% EtOAc/hexane) over silica afforded 250 mg (89%) of **7** as a white solid: mp = 65.0–65.8 °C; ^1H NMR; ^{13}C NMR; ^{31}P NMR; MS (FAB); Anal.

3,4-Dihydro-2-[(dimethoxyphosphinyl)methyl]-6-methyl-8-(4-methyl-1-oxobutyl)-2*H*-1-benzopyran, 8. To a stirring solution of 100 mg of **7** (0.36 mmol) and 68 μL of isovaleryl chloride (0.56 mmol) in 2.0 mL of nitromethane at 0 °C, under an argon atmosphere, was added 105 μL of titanium tetrachloride ($TiCl_4$). The reaction mixture was stirred for 30 min at 0 °C, allowed to warm to room temperature, and stirred an additional 2 h. The solution was cooled to 0 °C, treated with saturated $NaHCO_3$ (0.5 mL) and then diluted with 20 mL of H_2O and 20 mL of EtOAc. After stirring for 30 min, the resulting emulsion was centrifuged, and the aqueous layer was extracted with EtOAc (3 × 25 mL). The combined organic solutions were dried (Na_2SO_4) and concentrated to give a yellow oil. Flash chromatography (85% EtOAc/hexane) over silica yielded 108 mg (82%) of **8** as a yellow oil: IR, ^1H NMR; ^{13}C NMR, ^{31}P NMR; MS (FAB); Anal.

3,4-Dihydro-2-[(dimethoxyphosphinyl)methyl]-6-methyl-8-[4-methyl-1-(methoxyimino)butyl]-2*H*-1-benzopyran, 9. To a stirring mixture of 606 mg of **8** (1.7 mmol) in 9.0 mL of CH_3OH at room temperature was added 709 mg of $KHCO_3$ (5.1 mmol) and 607 mg of methoxyamine hydrochloride (7.3 mmol). The resulting mixture was refluxed for 2 h under a nitrogen atmosphere and then cooled to room temperature and filtered. The filtrate was concentrated to dryness and purified by flash chromatography (85% EtOAc/hexane) to yield 651 mg (99%) of **9** as a colorless oil and as a mixture of **2** diastereomers (approximately 60% *anti*: 40% *syn*): IR; ^1H NMR, ^{13}C NMR; ^{31}P NMR; MS (FAB); Anal.

3,4-Dihydro-2-[(dimethoxyphosphinyl)methyl]-6-methyl-8-[4-methyl-1-[[(phenylmethoxy)carbonyl]amino]butyl]-2*H*-1-benzopyran, (*R,*R**)-10 and (*R**,*S**)-10.** To a stirring solution of 11 g of **9** (28.7 mmol) in 300 mL of THF at 0 °C was added 145 mL of 1 M BH_3/THF (145 mmol). The solution was warmed to room temperature, then refluxed under argon for 16 h, then cooled to 0 °C, and treated with 300 mL of dry MeOH. This mixture was concentrated under reduced pressure to a colorless oil, which was dissolved in CH_3OH and concentrated under reduced pressure (5×) to a white solid. The solid was partitioned between Et_2O and cold 1 N H_2SO_4, and the organic layer was extracted with cold 1 N H_2SO_4. The combined aqueous layer was cooled to 0 °C, made basic with saturated NH_4OH, and extracted with CH_2Cl_2 (3 × 100 mL). The CH_2Cl_2 solution was first dried over $MgSO_4$, then over 3 Å molecular sieves at 0 °C for 24 h. To this solution was added 12.4 mL of triethylamine and 17.3 mL of benzyl chloroformate (CbzCl), and the resulting mixture was stirred for 8 h as it warmed to room temperature. The reaction mixture was concentrated and partitioned between H_2O and EtOAc, and the organic layer was dried ($MgSO_4$) and concentrated to a colorless oil. Flash chromatography (85% EtOAc/hexane) over silica yielded three fractions: 870 mg of (*R**,*R**)-**10**, 6 g of an (*R**,*R**)-**10** and (*R**,*S**)-**10** mixture, and 120 mg of (*R**,*S**)-**10** (50% total yield). (*R**,*R**)-**10**: IR; ^1H NMR; ^{13}C NMR; ^{31}P NMR. (*R**,*S**)-**10**: IR, ^1H NMR; ^{13}C NMR; ^{31}P NMR. (*R**,*R**)-**10** and (*R**,*S**)-**10** mixture: MS (FAB); HRMS (FAB); calcd for $C_{26}H_{36}NO_6P$, 490.2358, found, 490.2372.

3,4-Dihydro-2*R-[[methoxy(oxy)phosphinyl]methyl]-6-methyl-8-[4-methyl-1*R**-[[(phenylmethoxy)carbonyl]amino]butyl]-2*H*-1-benzopyran Sodium Salt, (*R**,*R**)-11.** Compound (*R**,*R**)-**10** (1.75 g, 3.57 mmol) was dissolved in 150 mL of freshly distilled *tert*-butylamine, and the resultant solution was refluxed under argon for 72 h. The solution was concentrated to a white solid, which was purified by anion exchange chromatography over Sephadex DEAE with a linear gradient from 1:1 CH_3OH/H_2O to 1:1 CH_3OH/1 M TBK buffer, followed by cation exchange chromatography (Dowex, Li^+ form) and lyophilization to give 1.62 g (93%) of (*R**,*R**)-**11** as a white solid: ^1H NMR; ^{13}C NMR; ^{31}P NMR; MS (FAB): HRMS (FAB); Calcd for $NaC_{25}H_{33}NO_6P$, 498.2021; found 498.2014.

3,4-Dihydro-2*R-[[methoxy(oxy)phosphinyl]methyl]-6-methyl-8-[4-methyl-1*S**-[[(phenylmethoxy)carbonyl]amino]butyl]-2*H*-1-benzopyran Sodium Salt, (*R**,*S*)-11.** As described above for the (*R**,*R**)-isomer, 2.0 g (4.09 mmol) of (*R**,*S**)-**10** was converted to 1.89 g (91% yield) of (*R**,*S**)-**11**: ^{1}H NMR; ^{13}C NMR; ^{31}P NMR; MS (FAB); HRMS (FAB); calcd for $NaC_{25}H_{33}NO_6P$, 498.2021, found, 498.2017.

***N*-[[[3,4-Dihydro-6-methyl-8-(3-methyl-1*R**-[[(phenylmethoxy)carbonyl]amino]butyl]-2*H*-1-benzopyran-2*R**-yl]methyl]methoxyphosphinyl]-L-leucine Phenylmethyl Ester, (*R**,*R**)-12.** The tosylate salt of leucine benzyl ester (3.0 g, 4.1 mmol) was mixed with 10 mL of EtOAc and 20 mL of 10% K_2CO_3. The aqueous layer was removed and the organic layer was washed with saturated NaCl, dried ($MgSO_4$), diluted with 5 mL of EtOAc, and placed over 3Å molecular sieves for 24 h. To this solution was added 13 mL of DIEA, and the resultant solution was cooled to −78 °C. To a stirred solution of 381 mg of (*R**,*R**)-**11** (0.75 mmol) in 7.6 mL of benzene and 150 μL of DMF under argon was added 145 μL of oxalyl chloride; extensive bubbling and formation of a white precipitate was observed. The reaction mixture was stirred for 15 min, then frozen, and lyophilized. The resultant solid was dissolved in benzene, under argon, frozen, and lyophilized once again. The resultant white solid was dissolved in 3.8 mL of CH_3CN and cooled to −20 °C under argon. To this mixture was added, via a cannula, the leucine benzyl ester/DIEA/EtOAc solution at −78 °C. The reaction mixture was stirred at −20 °C for 30 min, then warmed to room temperature, and stirred an additional 10 h. The reaction mixture was concentrated to a white oily solid, which was purified by flash chromatography over silica (twice; 90% EtOAc/hexane then 75% EtOAc/hexane) to give 365 mg (72%) of a colorless oil (*R**,*R**)-**12** (as a mixture of four diastereomers): IR; ^{1}H NMR; ^{31}P NMR; MS (FAB); HRMS (FAB); calcd for $C_{38}H_{51}N_2O_7P$, 679.3516, found, 679.3518.

***N*-[[[3,4-Dihydro-6-methyl-8-(3-methyl-1*R**-[[(phenylmethoxy)carbonyl]amino]butyl]-2*H*-1-benzopyran-2*S**-yl]methyl]methoxyphosphinyl]-L-leucine Phenylmethyl Ester, (*R**,*S**)-12.** As described above for the *R**,*R**-isomer, 294 mg (0.59 mmol) of (*R**,*S**)-**11** was converted to 205 mg of (*R**,*S**)-**12** (52% yield; four diastereomers): IR, ^{1}H NMR; ^{31}P NMR; MS (FAB): HRMS (FAB): calcd for $C_{38}H_{51}N_2O_7P$, 679.3516, found, 679.3514.

[2*R*-(2*R,6*S**,9*S**)]-3,4,5,6,8,9-Hexahydro-4-methoxy-11-methyl-6,9-bis(2-methylpropyl)-2,13-ethano-1,5,8,4-benzodiazaphosphacycloundecin-7(2*H*)-one-4-oxide, (*R*,*S*)-13, and the 2*S*,9*R*-Isomer (*S*,*R*)-13.** To a solution of 65 mg of (*R**,*S**)-**12** (0.1 mmol) and 30 mg of $NaHCO_3$ in 5 mL of degassed CH_3OH was added 20 mg of 5% Pd/C. The resultant mixture was stirred, at atmospheric pressure, under a H_2 atmosphere for 60 min. This mixture was filtered through a Millipore filter (0.45 μm pore size) and concentrated to a white solid. This solid was lyophilized from benzene to remove any residual CH_3OH, then dissolved in 12.5 mL of dry DMF, and cooled to −5 °C. The reaction mixture was stirred vigorously, and 100 μL of diphenyl phosphoryl azide (DPPA, 0.5 mmol) and 84 mg of solid $NaHCO_3$ (1 mmol) were added sequentially. At 24-h intervals, an additional 100 μL of DPPA and 42 mg of solid $NaHCO_3$ were added sequentially (two additional additions), while the vigorous stirring and −5 °C temperature were maintained. After 96 h, the reaction mixture was concentrated to a white solid. This material was dissolved in 10 mL of H_2O, and the aqueous mixture was extracted with EtOAc (3 × 20 mL). The combined organic layer was dried ($MgSO_4$) and concentrated to a white solid, which was purified by flash chromatography over silica (stepwise gradient: 2% CH_3OH/EtOAc, 5% CH_3OH/EtOAc, 10% CH_3OH/EtOAc, amd 20% CH_3OH/EtOAc) to give 5 mg of (*S*,*R*)-**13** (one diastereomer at phosphorus) and 17.2 mg of (*R*,*S*)-**13** (two diastereomers at phosphorus), both as white solids (51% total yield). (*R*,*S*)-**13**: IR, ^{1}H NMR; ^{31}P NMR; MS (FAB); HRMS (FAB); calcd for $C_{23}H_{37}N_2O_4P$, 437.2569, found 437.2579. (*S*,*R*)-**13**: IR; ^{1}H NMR; ^{31}P NMR; MS (FAB); HRMS (FAB); found, 437.2563.

[2*R*-(2*R,6*S**,9*R**)]-3,4,5,6,8,9-Hexahydro-4-methoxy-11-methyl-6,9-bis(2-methylpropyl)-2,13-ethano-1,5,8,4-benzodiazaphosphacycloundecin-7(2*H*)-one-4-oxide, (*R*,*R*)-13, and the 2*S*,9*S*-Isomer (*S*,*S*)-13.** As described above for cyclization of the (*R**,*S**)-isomer, 68 mg (0.1 mmol) of (*R**,*R**)-**12** was converted to 9.0 mg of (*R*,*R*)-**13** (one diastereomer at phosphorus) and 15 mg of (*S*,*S*)-**13** (two diastereomers at phosphorus), both as white solids (55% yield). (*R*,*R*)-**13**: ^{1}H NMR; ^{13}C NMR; ^{31}P NMR; MS (FAB): HRMS (FAB); calcd for $C_{23}H_{37}N_2O_4P$, 437.2569, found, 437.2564. (*S*,*S*)-**13**: ^{1}H NMR; ^{13}C NMR; ^{31}P NMR; MS (FAB); HRMS (FAB); found, 437.2567.

Enzymology General Methods. All stock solutions were prepared with doubly distilled water and filtered through Millipore filters (0.45 μm pore size). The standard buffer for all assays was 0.1 M 3-(*N*-morpholino)-propanesulfonic acid (MOPS), 2.5 M NaBr, 10 mM $CaCl_2$, and 2.5% (v/v) DMF at pH 7.0. Buffers were prepared and adjusted to pH at room temperature. Assays were performed on a Uvikon 860 spectrophotometer. A Lauda Model RM 20 circulating constant-temperature bath connected to a water-jacketed sample holder was used for temperature regulation (25 ± 0.2 °C). All inhibitors were shown to be free of any organic or phosphorus-containing impurities by high field ^{1}H and ^{31}P NMR spectroscopy. Concentration of inhibitors (*R*,*S*)-**1** and control compounds **2** and **3** were determined by careful dilution of a precisely weighed sample of the inhibitor and correction for the percent phosphorus detd. by elemental analysis. Concentrations of inhibitors (*S*,*S*)-**1**, (*R*,*R*)-**1**, and (*S*,*R*)-**1** were determined by UV absorbance based on the ε value determined for (*R*,*S*)-**1**. Thermolysin was obtained from Cal Biochem (3× recrystallized) and used without further purification. Enzyme concentration was determined by UV absorbance and was between 10 and 20 nM. The thermolysin substrate furanacryloyl-glycyl-leucinamide (faGLa) was obtained from Sigma and used without further purification. Stock substrate concentration was determined by UV absorbance (ϵ_{345} 766). Assays were performed at 25 °C, monitored by absorbance change at 345 nm, and followed for ≤10% of the total reaction.

Kinetic Parameters for Thermolysin Hydrolysis of Furanacryloyl-Glycyl-Leucinamide. Assays were carried out with 10–20 nM thermolysin and 0.10–8.0 mM faGLa. Short pathlength cells (2 and 5 mm) were used for the higher concentrations of substrate to keep the total absorbance of the solution below 2.5 AU. At each concentration of substrate, the difference in molar extinction coefficient ($\Delta\epsilon$ = 345) was determined and shown to vary by less than 8%.

Determination of K_i's. The assay was initiated by the addition of faGLa (2 mM) and differences in molar extinction coefficients ($\Delta\epsilon$ = 345) measured. All velocities were determined for ≤10% reaction and were reproducible within ±8%. Inhibitors (*S*,*S*)-**1**, (*R*,*S*)-**1**, (*R*)-**2**, and (*S*)-**2** were initially dissolved in methanol at concentrations around 0.01 M and then diluted to stock concentrations (1×10^{-5}–5×10^{-7} M) with assay buffer. The K_i values for (*S*,*S*)-**1**, (*R*,*S*)-**1**, **3**, (*R*)-**2**, and (*S*)-**2** were determined from v_o/v_i versus [I] plots ($v_o/v_i = [I]/K_i(1 + [S]/K_m) + 1$) with six or more different concentrations of I over a range of at least $^1/_2 \times K_i$ to $10 \times K_i$. For (*S*,*S*)-**1**, the data were also analyzed by the method of Henderson[37] to ensure that inhibitor depletion at low [I] did not lead to an overestimation of the K_i value obtained. The kinetic plots are reproduced in the supplementary material.

Crystallography. Thermolysin (Calbiochem) was crystallized[25] and stored in a mother liquor (M7) comprised of 0.01 M calcium acetate, 0.01 M Tris-acetate, and 7% (v/v) dimethyl sulfoxide, pH 7.25. Crystals of the thermolysin–inhibitor complexes were formed by soaking the native crystals in solutions of the inhibitor in M7. The extent of binding was assessed by calculating (*hOl*) difference density projections between the native crystals and the inhibitor complex.[38] Optimal binding for each inhibitor, coupled with minimal crystal cracking, required slow equilibration (over 2 days) of a thermolysin crystal to a final inhibitor concentration of 1 mM, followed by an additional soaking period of 3 days.

The same data collection strategy was used for both inhibitor complexes. In each case, a single crystal was used to collect three-dimensional data on a Xuong–Hamlin area detector[39] using graphite-monochromated CuK_α radiation from a Rigaku RU200 rotating anode generator. Intensity statistics are given in Table 2.

The initial electron density maps for each inhibitor complex are shown in Figure 5a,b. A complete starting model for each inhibitor molecule was built into the initial map based on the positive 3σ density and used in subsequent refinement. In both cases, this map clearly outlined the shape and position of the inhibitor bound within the active site cleft. Positions for all the atoms of inhibitor (*S*)-**2** were well defined in this initial map. Although inhibitor (*S*,*S*)-**1** was initially somewhat less well defined in the vicinity of each of the leucine side chains (Figure 5a), these regions were quite clear in the final ($2F_{PI}$–F_C) map using the fully refined model (not shown).

Each protein–inhibitor complex model was refined using the TNT package.[40] Both thermal factors and coordinates were refined simultaneously, starting with relaxed geometry and later increasing the constraints to impose expected stereochemistry. Each "residue" of each inhibitor was successively omitted from the model prior to a round refinement, and the resulting (F_{PI}–F_C) difference map was used to verify or adjust the position of each of the corresponding atoms. No inhibitor atoms proved to be troublesome to fit. A ($2F_{PI}$–F_C) map calculated using the fully refined models showed continuous density covering all inhibitor atoms at 1σ. With an average of approximately 15Å^2 for both inhibitors, final thermal factors suggest that each inhibitor is well localized

in the active site with mobility comparable to the protein atoms in the same vicinity. Once an inhibitor was fully refined, well-ordered water molecules were added back into the active site region of the model at positions suggested by the difference electron density maps. A final crystallographic *R*-factor of 16.8% was achieved for each model (Table 2). Coordinates have been deposited in the Brookhaven Protein Data Bank.

Acknowledgment. Support for this work was provided by the National Institutes of Health through Grants GM-30759 (to P.A.B.), GM-20066 (to B.W.M), and Training Grant GM-07759, and the Regents of the University of California through a fellowship to B.P.M. We also thank the members of the Computer Graphics Facility of the University of California, San Francisco, for their assistance in molecular modeling in the early stages of the project.

Supplementary Material Available: Spectral characterization of diastereomers of **1**, synthesis and characterization of control compounds **2** and **3**, and kinetic analysis of inhibition experiments (13 pages). This material is contained in many libraries on microfiche, immediately follows this article in the microfilm version of the journal, and can be ordered from the ACS; see any current masthead page for ordering information. The X-ray coordinates of the complexes of thermolysin with (*S*,*S*)-**1** and (*S*)-**2** have been deposited with the Brookhaven Protein Databank.